Astron. Astrophys. 353, 498–506 (2000)

ASTRONOMY AND ASTROPHYSICS

# *Beppo*SAX observations of two high redshift clusters of galaxies: RXJ 0152.7−1357 and MS 2053.7−0449

**R. Della Ceca**[1], **R. Scaramella**[2], **I.M. Gioia**[3,4], **P. Rosati**[5], **F. Fiore**[2,6], **and G. Squires**[7,8]

[1] Osservatorio Astronomico di Brera, via Brera 28, 20121 Milano, Italy
[2] Osservatorio Astronomico di Roma, via Frascati 33, 00040 Monteporzio Catone, Italy
[3] Institute for Astronomy, 2680 Woodlawn Drive, Honolulu, HI 96822, USA
[4] Istituto di Radioastronomia del CNR, via Gobetti 101, 40129 Bologna, Italy
[5] European Southern Observatory, 85748 Garching bei München, Germany
[6] BeppoSAX Science Data Center, via Corcolle 19, 00131 Roma, Italy
[7] Center for Particle Astrophysics, UC Berkeley, 301 Le Conte Hall, Berkeley, CA, USA
[8] Caltech Astronomy M/S 105-24, 1200 E. California Blvd., Pasadena, CA, USA

Received 4 August 1999 / Accepted 20 October 1999

**Abstract.** We present X-ray observations of two high redshift clusters of galaxies carried out with the *Beppo*SAX satellite. One cluster, RXJ 0152.7−1357 at $z \simeq 0.83$, was selected from the ROSAT Deep Cluster Survey sample, as one of the most X-ray luminous systems known at $z > 0.5$. The optical and ROSAT-PSPC data show a complex morphology with at least two cores. Our SAX observations yield a gas temperature $kT = 6.46^{+1.74}_{-1.19}$ keV and a metallicity $A = 0.53^{+0.29}_{-0.24}$, with a prominent iron $K_\alpha$ line. The second cluster, MS 2053.7−0449 at $z \simeq 0.58$, was selected from the EMSS sample. Given the poor statistics no constraints on the metallicity can be derived from the present data. Large uncertainties are associated to the gas temperature ($kT = 6.7^{+6.8}_{-2.3}$ keV), which has been obtained after fixing the abundance to 0.3 solar. Combining these results with those obtained for similarly high redshift ($z \geq 0.5$) clusters of galaxies with broad band X-ray spectra, we discuss the high redshift $L_{bol} - T$ relationship. The data can easily be accommodated with a non-evolving (or mildly evolving) $L_{bol} - T$ relation, a result which, when combined with the little observed evolution in the bulk of the X-ray cluster population, gives support to low $\Omega$ cosmological models.

**Key words:** galaxies: clusters: individual: MS 2053.7-0449 – galaxies: clusters: individual: RXJ 0152.7-1357 – cosmology: observations – X-rays: galaxies

## 1. Introduction

High redshift clusters of galaxies have long served as valuable tools to test theories of cosmic structure formation (e.g. Press and Schechter 1974, Peebles et al. 1989, Eke et al. 1996, to mention just a few). Measurements of the temperature of the intra-cluster medium (ICM) in distant clusters are particularly important since cluster temperatures are closely related to their mass, as long as these systems are in virial equilibrium. Physical cluster parameters of the highest redshift clusters, measurable by means of deep X-ray observations (e.g. the Luminosity-Temperature relation), set also strong constraints on the thermodynamical evolution of their gaseous component. In addition, the measurement of the metal abundance from X-ray spectra in remote bound systems can constrain the mode and epoch of the enrichment of the intracluster gas.

Despite their importance, ICM properties at high redshift ($z > 0.5$) are still largely unexplored. This is due to the limited effective area and spatial resolution of the past X-ray missions, as well as to the difficulty of finding X-ray luminous clusters at $z > 0.5$. Indeed the *Extended Medium Sensitivity Survey* (EMSS; Gioia et al., 1990) carried out with the Einstein Observatory has detected clusters at redshift up to $\sim 0.8$ (e.g. MS1137+6625 at 0.78 and MS1054-0321 at z=0.83, Gioia & Luppino, 1994; Donahue et al., 1998) but the statistics of high-z clusters in the EMSS is still low with only 6 clusters (out of a total of about 100) at $z > 0.5$. Over the last few years, however, several X-ray cluster surveys based on ROSAT-PSPC data (the RDCS: Rosati et al., 1995, 1998; the WARPS: Scharf et al., 1997; the SHARC: Burke et al., 1997; the 160° survey of Vikhlinin et al., 1998; the NEP: Mullis et al., 1998) have changed the observational scenario by collecting sizable samples of distant ($z > 0.5$) systems, thus extending the pioneering work of the EMSS. The ROSAT Deep Cluster Survey (RDCS, Rosati et al. 1995, 1998) has pushed these studies to the faintest fluxes and highest redshifts, with 33 clusters spectroscopically identified to date at $z > 0.5$, out to $z = 1.26$ (Rosati et al. 1999).

As an alternative method, several studies have tried to locate distant clusters around high redshift radio galaxies (e.g. 3C 324 at $z = 1.2$, Smail & Dickinson, 1995; 3C 184 at $z = 0.99$, Deltorn et al. 1997). ROSAT observations of distant radio galaxies (Crawford & Fabian 1996; Dickinson 1997) have provided some evidence that the observed X-ray emission might originate from hot intra-cluster gas. It remains difficult, however, to reli-

*Send offprint requests to*: R. Della Ceca (rdc@brera.mi.astro.it)

**Table 1.** Observed clusters

| Name | RA (J2000) | DEC (J2000) | z | Energy Band keV | $f_x$ [a] erg cm$^{-2}$ s$^{-1}$ | $L_x$ [a] h$_{50}^{-2}$ erg s$^{-1}$ |
|---|---|---|---|---|---|---|
| RXJ 0152.7−1357 | 01 52 41 | -13 57 45 | 0.831 | 0.5 − 2.0 | $2.2 \pm 0.2 \times 10^{-13}$ | $6.8 \pm 0.6 \times 10^{44}$ |
| MS 2053.7−0449 | 20 56 22 | -04 37 52 | 0.583 | 0.3 − 3.5 | $4.0 \pm 0.9 \times 10^{-13}$ | $5.8 \pm 1.3 \times 10^{44}$ |

[a] We note that in the case of RXJ 0152.7−1357 we have reported the ROSAT PSPC flux$_{(0.5-2.0\ keV)}$ (luminosity) measured over a circle of 3 arcmin radius, corresponding to $1.5 h_{50}^{-1}$ Mpc at $z = 0.83$, while for MS 2053.7−0449 we have reported the total EMSS "corrected" flux$_{(0.3-3.5\ keV)}$ (luminosity) i.e. the flux (luminosity) corrected for the effect of the finite EMSS detection cell.

**Table 2.** *Beppo*SAX data observation journal

| Name | Date | Seq. Numb | Exp. LECS ksec | Rate LECS ($10^{-3}$ cts s$^{-1}$) (0.12 − 4.0 keV) | Exp. MECS ksec | Rate MECS ($10^{-3}$ cts s$^{-1}$) (1.65 − 10 keV) |
|---|---|---|---|---|---|---|
| RXJ 0152.7−1357 | 1998 Aug 7-10 | 60605001 | 61.3 | $2.7 \pm 0.3$ | 127.7 | $4.0 \pm 0.3$ |
| MS 2053.7−0449 | 1997 Oct 21-23 | 60243001 | 32.7 | $2.7 \pm 0.4$ | 81.9 | $2.4 \pm 0.3$ |

ably measure ICM physical parameters in these objects, since one needs to discriminate an absorbed power-law component, due to the radio galaxy's AGN, from the thermal component of the putative diffuse ICM.

Although the number of *bona-fide* high-$z$ clusters has significantly increased, only long ASCA observations, with a broad energy response, have allowed a few sketchy studies of their ICM properties to date. A recent compilation of cluster temperatures (Wu et al. 1999) reports a total of 168 clusters with good broad band X-ray spectroscopy, but only 5 (3) of these have been studied at $z > 0.5$ ($z > 0.8$).

In this paper we present *Beppo*SAX observations of two high redshift clusters: MS 2053.7−0449 from the EMSS sample at $z = 0.583$ and RXJ 0152.7−1357 from the RDCS sample at $z = 0.831$. The *Beppo*SAX MECS instrument (see Sect. 2) has a slightly smaller (larger) effective area than the ASCA GIS for $E < 7$ keV ($E > 7$ keV) and it is characterized by a significantly sharper PSF if compared with the ASCA GIS or ASCA SIS instruments, especially at high energy. This latter property implies a reduced background, making *Beppo*SAX MECS the best instrument to date for distant clusters investigations. RXJ 0152.7−1357 is the highest redshift cluster with good quality broad band X-ray spectroscopy to date and among the most X-ray luminous known at $z > 0.6$ together with the well known MS1054.4−0321 (Gioia & Luppino, 1994; Donahue et al., 1998). Our data provide a rather accurate ($\sim 20\%$) temperature measurement for RXJ 0152.7−1357, which allows an interesting comparison with MS1054.4−0321 with very similar redshift and luminosity. In Table 1 the main properties of the two clusters, in their own discovery bands, are summarized.

This paper is organized as follows. In Sect. 2 we present the *Beppo*SAX observations. The spectral analysis for RXJ 0152.7−1357 is presented in Sect. 3 and for MS 2053.7−0449 in Sect. 4. Sect. 5 contains a discussion of the results in the context of the high redshift $L_{bol} - T$ relationship. Finally, summary and conclusions are presented in Sect. 6. We adopt $H_0 = 50$ km s$^{-1}$ Mpc$^{-1}$ and $q_0 = 0.5$ throughout, unless otherwise noted.

## 2. *Beppo*SAX observations and data preparation

The observations were performed with the *Beppo*SAX Narrow Field Instruments, LECS (0.1–10 keV, Parmar et al. 1997), MECS (1.3–10 keV, Boella et al. 1997), HPGSPC (4–60 keV, Manzo et al. 1997) and PDS (13–200 keV, Frontera et al. 1997). We report here the analysis of the imaging instruments data (LECS and MECS). PDS and HPGSPC are collimated instruments with field of view of about 1.5 degrees (FWHM) and have a rather large and structured background which makes them not sensitive enough for very faint sources.

At launch the MECS was composed of three identical units. Unfortunately on 1997 May $6^{th}$ the unit MECS1 had a technical failure. All observations after this date were performed with two units (MECS2 and MECS3). The LECS is operated during spacecraft dark time only, therefore LECS exposure times are usually smaller than MECS exposures by a factor 1.5–3. The MECS energy resolution is about 8% at 6 keV, while the LECS energy resolution is about 11% at 3 keV.

Table 2 gives the journal of observations for the two high redshift clusters. For both clusters we have acquired $\approx 30\%$ fewer photons than anticipated (because of the unavailability of one of the three MECS in the case of MS $2053.7.7 - 0449$, and because of the shorter effective exposure in the case of RXJ 0152.7−1357).

Standard data reduction was performed using the software package "SAXDAS" (see http://www.sdc.asi.it/software and Fiore et al. 1999). In particular, data are linearized and cleaned from Earth occultation periods and unwanted periods of high particle background (satellite passages through the South Atlantic Anomaly). We accumulated data for Earth elevation angles $> 5$ degrees and magnetic cut-off rigidity $> 6$. Data from the two MECS units have been merged after gain equalization and single MECS spectra have been accumulated.

Both MECS and LECS source counts have been extracted from a circular region of 4 arcmin radius to maximize the statistics and the signal-to-noise (S/N) ratio.

LECS and MECS internal backgrounds depend on the position of the target in the detector (see Chiappetti et al. 1998, the *Beppo*SAX Cookbook, http://www.sdc.asi.it/software/cookbook and Parmar et al. 1999). Accordingly, background spectra were extracted from high Galactic latitude "blank" fields from the same source extraction region, in detector coordinates. The mean level of the background in the "blank fields" was compared with that of our observations using source-free regions at various positions in the detectors. The level of the "blank fields" background is consistent with the "local" background in the two cluster observations.

Spectral fits were performed using the XSPEC 9.0 software package and the September 1997 version of the calibration files (Ancillary Response Files and Redistribution Matrix Files). In the spectra analysis only the 1.65−10 keV band counts for the MECS (channels 37 − 220) and the 0.12−4 keV counts for the LECS (channels 11 − 400) were used as suggested by the *Beppo*SAX Cookbook (Fiore et al. 1999, v. 1.2). The background subtracted count rates ($\pm 1\sigma$) in both LECS (0.12–4 keV) and MECS (1.65–10 keV) are given in Table 2. Source counts were binned in order to have a S/N $\geq 3$ in each energy bin. The LECS and MECS data were fitted jointly, and the model normalization for each data set were allowed to be an independent parameter, in order to take into account differences in the absolute calibration of the two instruments. If not explicitly quoted all the errors reported in this paper represent the $68\%$ confidence levels for 1 interesting parameter ($\Delta\chi^2$ = 1.0).

## 3. RXJ 0152.7−1357

RXJ 0152.7−1357 was discovered in the RDCS which has constructed an X-ray selected, flux-limited sample of clusters of galaxies via a serendipitous search for extended X-ray sources in deep pointed PSPC observations. A wavelet-based technique was employed to characterize low-surface brightness sources and select cluster candidates down to the flux limit $f_{0.5\text{–}2.0\,keV}$ of $1 \times 10^{-14}$ erg cm$^{-2}$ s$^{-1}$, over $\sim 50$ deg$^2$ (Rosati et al., 1995). Optical follow-up imaging and spectroscopy have confirmed to date $\sim 140$ clusters and groups, which span a large range in redshift [0.05–1.26] and X-ray luminosity [$1 \times 10^{42} - 8 \times 10^{44} h_{50}^{-2}$ erg s$^{-1}$], RXJ 0152.7−1357 being the most luminous of the sample.

RXJ 0152.7−1357 was discovered in the ROSAT PSPC field rp600005n00 pointed at the nearby galaxy NGC 720. The cluster was detected at 13.6′ off-axis ($\alpha_{2000} = 01^h52^m41^s$ and $\delta_{2000} = -13^o57'45''$). At this position the wavelet algorithm clearly reveals an extended X-ray source with an extent $6.5\sigma$ above the local PSF of the ROSAT PSPC instrument and with a double core (the multi-scale wavelet analysis preserves source substructure information) with intensity peaks separated by $\sim$ 1.2 arcmin ($\sim 0.6 h_{50}^{-1}$ Mpc at the cluster redshift of $z = 0.83$). This same cluster has also independently been identified in the WARPS survey (Ebeling et al. 1999) and recently reported also in Romer et al. (1999).

Integrating the ROSAT PSPC flux over a circle of 3 arcmin radius, corresponding to $1.5 h_{50}^{-1}$ Mpc at $z = 0.83$, we obtain $377 \pm 27$ net counts[1] in the 0.5–2.0 keV energy band, with 6.2/arcmin$^2$ background counts. With an effective exposure time of 19904 sec, a galactic HI column density along the line of sight of $1.55 \times 10^{20}$cm$^{-2}$ (Dickey & Lockman 1990) and using a Raymond-Smith spectral model (Raymond & Smith 1977) with kT $\sim$ 6 keV, we obtain an unabsorbed flux of $f_{0.5-2.0\,keV} = (2.2 \pm 0.2) \times 10^{-13}$ erg cm$^{-2}$ s$^{-1}$. The rest frame X-ray luminosity within an aperture of $1.5 h_{50}^{-1}$ Mpc is $L_X = (6.8 \pm 0.6) \times 10^{44} h_{50}^{-2}$ erg s$^{-1}$.

Imaging and spectroscopic follow-up observations of RXJ1052.7−1357 were conducted with the EFOSC1 spectrograph at the ESO 3.6m in November 1996. With a long slit exposure of 2 hours it was possible to secure redshifts for 3 galaxies with $\langle z \rangle \simeq 0.831$ belonging to the main northern clump. Additional multiband imaging and spectroscopy have been carried out at Keck with the Low Resolution Imaging Spectrograph (LRIS, Oke et al., 1995) and are presented and discussed elsewhere (Squires et al. in preparation), along with a weak lensing analysis of the field. We only note here that the new spectroscopic data confirm the redshift of $z \sim 0.83$ also for the southern clump.

In Fig. 1, we show the R-band image (obtained with Keck-LRIS; 4000 s integration time) with the PSPC X-ray contours overlaid. The cluster galaxies distribution shows two main clumps and correlates very well with the double-peaked X-ray morphology.

The *Beppo*SAX - MECS X-ray image of the field in the 2–10 keV band is shown in Fig. 2. The source, centered at $\alpha_{2000} = 01^h52^m41^s$ and $\delta_{2000} = -13^o57'23''$, is consistent with the celestial position of the cluster within the SAX positional errors. This source is marginally resolved at the spatial resolution of the *Beppo*SAX - MECS.

The total net counts in the source extraction region are $165 \pm 17$ for the LECS and $506 \pm 36$ for the MECS. The net counts represent about 59% (39%) of the total (source + background) counts in the source region for LECS (MECS).

The source spectrum was fitted using a Raymond-Smith spectral model modified by galactic absorption ($N_H = 1.55 \times 10^{20}$ cm$^{-2}$) along the line of sight at the cluster position. The results are reported in Table 3. The cluster gas is best fitted by a rest frame temperature of $kT = 6.46^{+1.74}_{-1.19}$ and metallicity of $A = 0.53^{+0.29}_{-0.24}$ (68% confidence interval). The ratio of the model normalizations from LECS and MECS is about 0.71, which is consistent with the known differences in the absolute calibration of the two instruments.

[1] The south-west faint source, visible in Fig. 1 ($\Delta\alpha \sim 1.9'$ and $\Delta\delta \sim -1.8'$), possibly an AGN, was masked out in this measurement (this would increase the flux by 7%). The ROSAT hardness ratio map indicates that the spectra of this faint source is steeper than that of RXJ 0152.7−1357; therefore its contribution to the *Beppo*SAX data at $E > 1$ kev is below a few percents. An even smaller contribution is expected from the two bright stars visible in the south-east section of the image.

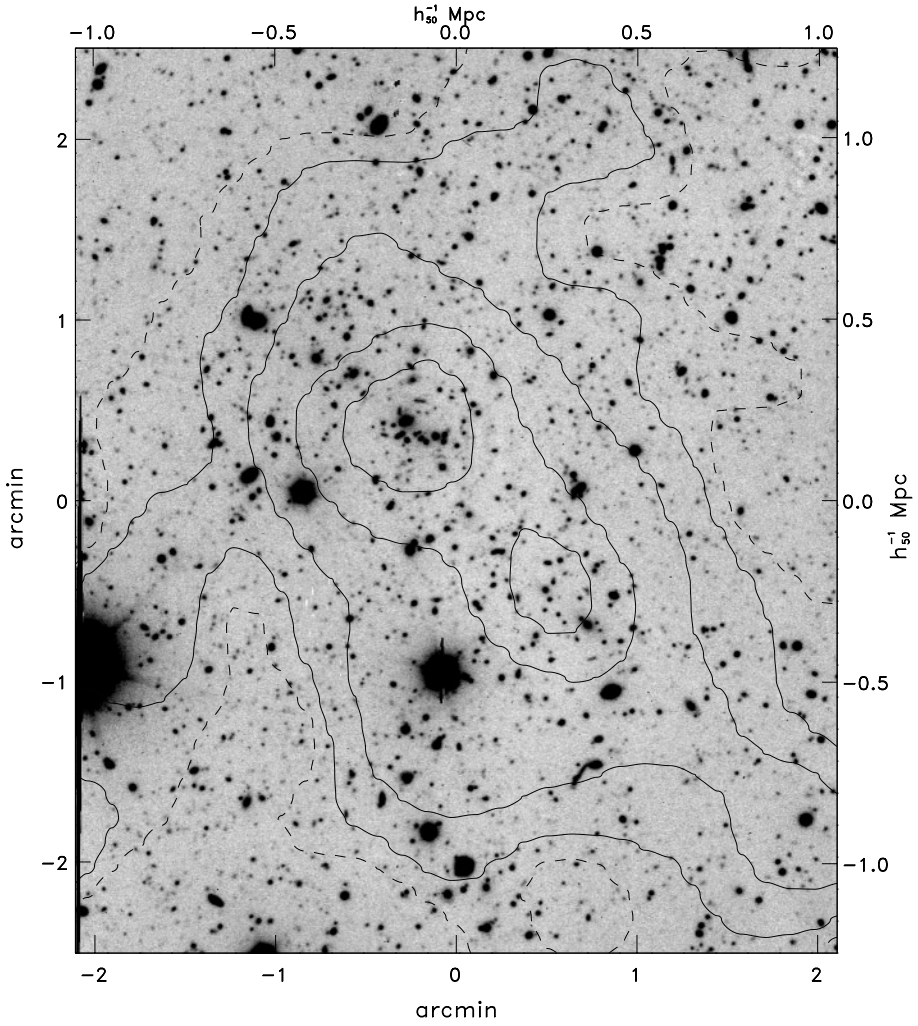


**Fig. 1.** R band image of RXJ1052.7−1357 with overlaid ROSAT PSPC X-ray contours at 3 (dashed line), 5, 10, 20 and 30 $\sigma$ above the background. The image was obtained with Keck-LRIS with 4000 s integration time (Squires et al. in preparation). The right and top axes give the physical linear scale at $z = 0.831$. The center coordinates are $\alpha_{2000} = 01^h52^m41^s$; $\delta_{2000} = -13^o57'45''$; north is up, east to the left.

**Table 3.** Results of the Spectral Fit (LECS+MECS): Raymond-Smith Thermal Model.

| Name | z | $N_{H_{Gal.}}$ ($10^{20}$ cm$^{-2}$) | KT (keV) | Abundance (Solar Units) | Norm. (LECS/MECS)[a] ($10^{-4}$) | $\chi^2_\nu$/dof |
|---|---|---|---|---|---|---|
| RXJ 0152.7−1357 | 0.831 | 1.55 (fixed) | $6.46^{+1.74}_{-1.19}$ | $0.53^{+0.29}_{-0.24}$ | $6.9^{+0.9}_{-0.8}/9.7^{+1.7}_{-1.5}$ | 0.79/21 |
| MS 2053.7−0449 | 0.583 | 4.96 (fixed) | $6.7^{+6.8}_{-2.3}$ | 0.3 (fixed) | $5.4^{+1.1}_{-0.9}/4.8^{+1.6}_{-1.1}$ | 0.93/7 |

*Note:* Errors are the 68% confidence interval for one interesting parameter ($\Delta\chi^2 = 1.0$).
[a] Normalization at 1 keV. This number is equal to $[10^{-14}/(4\pi D^2)] \int n_e^2 dV$, where D is the distance to the source in cm, $n_e$ is the electron density in units of cm$^{-3}$ and V is the volume filled by the X-ray emitting gas in cm$^3$

The unfolded spectrum, the folded spectrum and the ratio between the data and best fit model are displayed in Fig. 3, while in Fig. 4 we report the two-parameter $\chi^2$ contours (68.3%, 90% and 99% confidence levels) for the cluster metallicity (in solar units) and temperature (in keV). Both temperature and metal abundance are rather well constrained, which is partially due to the detection of the iron $K\alpha$ complex at the redshifted energy of about 3.7 keV. It is worth noting that leaving the redshift, along with the metallicity and temperature, as free parameters we obtain best fit values ($\chi^2_\nu/dof = 0.82/20$) of $z = 0.80^{+0.07}_{-0.05}$, $kT = 6.16^{+1.93}_{-1.08}$ and metallicity $A = 0.53^{+0.29}_{-0.24}$ (68% confidence interval). Finally, we have also tried a fit with the absorbing column density as a free parameter. We obtain best fit values ($\chi^2_\nu/dof = 0.84/19$) of $kT = 5.98^{+1.68}_{-1.37}$, $A = 0.51^{+0.27}_{-0.23}$ and $z = 0.81^{+0.06}_{-0.06}$; the best fit absorbing column density converges to zero with a $1\sigma$ upper limit of $2.4 \times 10^{21}$ cm$^{-2}$. These results confirm the robustness of our spectral fit.

Using the best fit model parameters reported in Table 3 and assuming a mean value between the LECS and MECS normalizations, we derive an unabsorbed (0.5–2.0) keV flux of $f_{0.5-2\,keV} = (1.9 \pm 0.4) \times 10^{-13}$ erg cm$^{-2}$ s$^{-1}$. The measured flux is in good agreement with that derived from the ROSAT PSPC data (see Table 1).

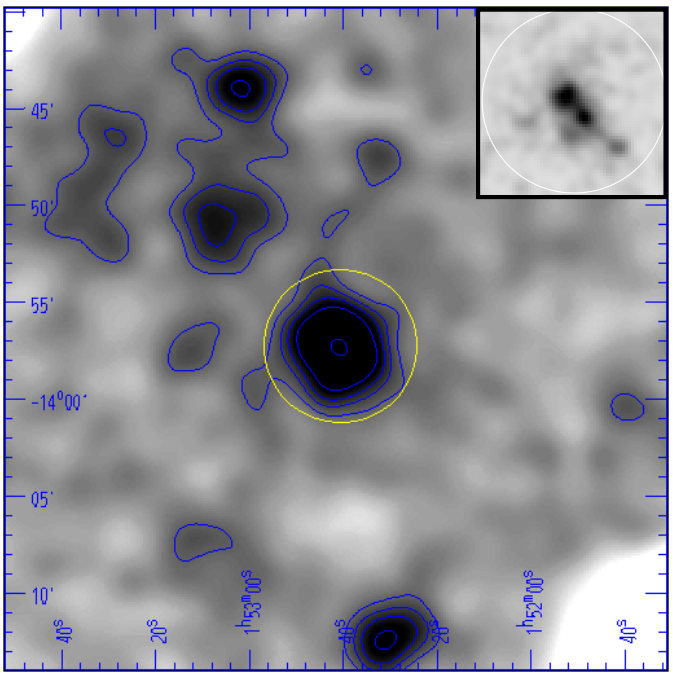


**Fig. 2.** MECS image in the 2–10 keV band of the RXJ 0152.7−1357 field ($35' \times 35'$). The raw data have been smoothed with a gaussian filter with $\sigma = 0.8'$. Contours are at 3, 5, 7, 10 and 20 sigma above the background. The white $4'$ radius circle represents the *Beppo*SAX counts extraction region for RXJ 0152.7−1357. The inset shows the ROSAT-PSPC cutout of the same central region in the [0.5–2.0] keV band, smoothed with a gaussian with $\sigma \simeq 14''$. The inset clearly shows the double core nature of RXJ 0152.7−1357.

The derived unabsorbed (2–10) keV flux is $f_{2-10\,keV} = (2.3 \pm 0.5) \times 10^{-13}$ erg cm$^{-2}$ s$^{-1}$, corresponding to a luminosity in the cluster rest frame of $L_{2-10\,keV} = (1.1 \pm 0.2) \times 10^{45} h_{50}^{-2}$ erg s$^{-1}$, and to a bolometric luminosity of $L_{bol} = (2.2 \pm 0.5) \times 10^{45} h_{50}^{-2}$ erg s$^{-1}$.

Given the uncertain dynamical state of RXJ0152.7-1357 and the difficulty in measuring its gas density profile, it is difficult to provide an accurate estimate of its mass[2].

## 4. MS 2053.7−0449

MS 2053.7−0449 is part of the EMSS sample of high-$z$ clusters of galaxies ($z > 0.5$) serendipitously discovered in the fields of the Einstein IPC. The X-ray source is located at $\alpha_{2000} = 20^h 56^m 22^s$ and $\delta_{2000} = -04^o 37' 52''$ and the unabsorbed IPC flux, corrected for the effect of the finite EMSS detection cell is $f_{0.3-3.5\,keV} = (4.0 \pm 0.9) \times 10^{-13}$ erg cm$^{-2}$ s$^{-1}$ (Henry et al. 1992; Gioia & Luppino 1994). The redshift of $z = 0.583$ is based on 5 concordant galaxy redshifts (Fabricant, private communication).

[2] Assuming the gas in isothermal and hydrostatic equilibrium the total mass within a radius $r (r \gg r_c)$ would be:

$$M(<r) \simeq 10^{15} \left(\frac{T}{6.5\,\mathrm{keV}}\right) \left(\frac{r}{\mathrm{Mpc}}\right) \left(\frac{\beta}{0.7}\right) h_{50}^{-1} M_\odot$$

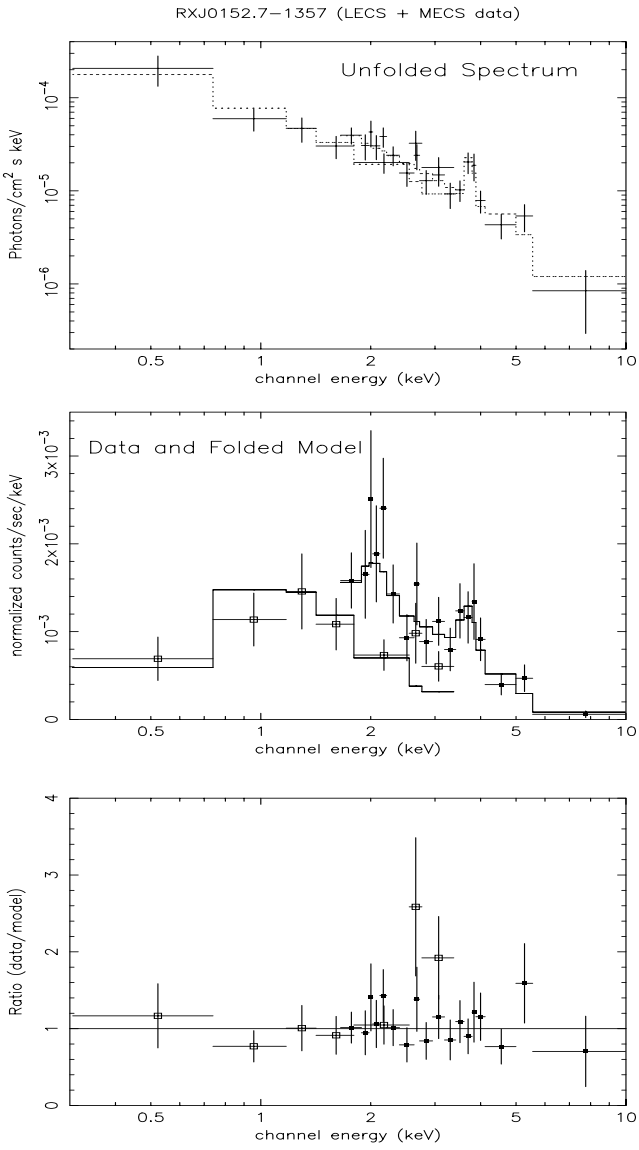


**Fig. 3.** RXJ 0152.7−1357: Unfolded spectrum, folded spectrum and the ratio between the data and best fit model. In the last two panels we have indicated the LECS (MECS) data as open (filled) squares. A prominent iron $K_\alpha$ complex at the redshifted energy of $\sim 3.7$ keV is visible.

Given its high luminosity, $L_{0.3-3.5\,keV} = (5.8 \pm 1.3) \times 10^{44} h_{50}^{-2}$ erg s$^{-1}$, MS 2053.7−0449 was part of the CCD imaging survey for gravitational lensing carried out with the telescopes at Mauna Kea by Luppino et al. (1999). Luppino & Gioia (1992) first reported the presence of a large arc (arc-length $\sim 11''$) fragmented into two distinct clumps at a radius of $\sim 16''$ from the optically dominant cluster galaxy.

A weak lensing study (Clowe 1998) shows that MS 2053.7−0449 is not among the most massive z$\sim$ 0.55 clusters of the EMSS. Clowe et al. (1999) report a mass value, from the weak lensing, of $(2.3 \pm 1.1) \times 10^{14} h_{100}^{-1} M_\odot$ within 0.5 $h_{100}^{-1}$ Mpc. The mass profile is well fit by a "universal" CDM profile (Navarro et al. 1996) with parameters $r_{200}$=590 $h_{100}^{-1}$

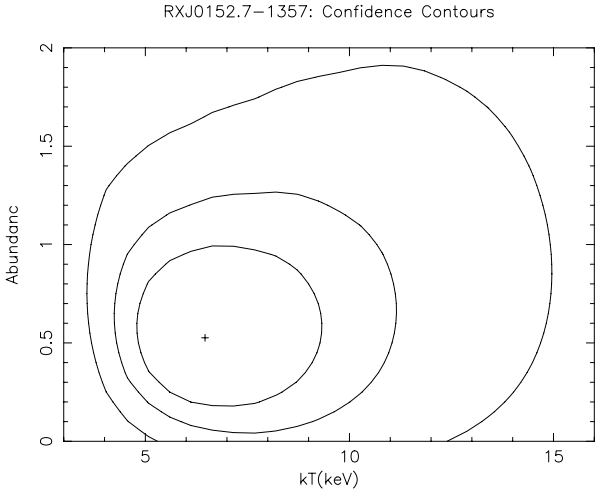


**Fig. 4.** RXJ 0152.7−1357: Two dimensional $\chi^2$ contours at 68.3%, 90% and 99% confidence levels ($\Delta\chi^2$ = 2.3, 4.61 and 9.21) for the cluster abundance (solar units) and temperature (in keV).

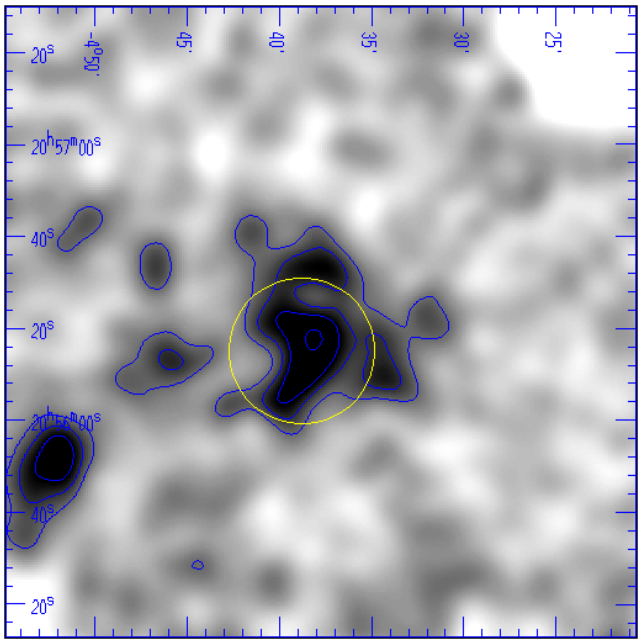

**Fig. 5.** MECS image in the 2–10 keV band of the MS 2053.7−0449 field ($35' \times 35'$). The raw data have been smoothed with a two-dimensional gaussian filter with $\sigma = 0.8'$. Contours are at 3, 5, 7, 10 and 20 sigma above the background. The white circle represents the counts extraction region for MS 2053.7.7−0449 (radius= $4'$).

kpc and c=2 assuming a background galaxy redshift $z_{bg}$=1.5. MS 2053.7−0449 is also well fit by an isothermal sphere model with a velocity dispersion of $\sigma = 730\,\mathrm{km\,s^{-1}}$ for $z_{bg}$=1.5, indicating that the cluster is close to virialization. Kelson et al. (1997) find that the fundamental plane relation of galaxies in MS 2053.7−0449 is very similar to that of Coma, suggesting that the structure of the early-type galaxies has changed little since $z = 0.58$.

The MECS 2–10 keV X-ray image of the field is shown in Fig. 5; the peak of the X-ray emission from the cluster is centered at $\alpha_{2000} = 20^h56^m21^s$ and $\delta_{2000} = -04^o38'53''$, which is consistent with the celestial position of the cluster within the SAX positional errors. The total net counts from MECS (LECS) are $200 \pm 24$ ($88 \pm 14$) and represent about 36% (47%) of the total (source + background) gross counts in the source region.

Table 3 reports the results of the spectral analysis. The source spectrum was fitted using a Raymond-Smith spectral model modified by galactic absorption ($N_H = 4.96 \times 10^{20}\,\mathrm{cm^{-2}}$, Dickey & Lockman 1990) along the line of sight at the cluster position. From the present data no constraints can be set on the abundance which was thus fixed to 0.3 solar. The cluster gas is best fit by a rest frame temperature $kT = 6.7^{+6.8}_{-2.3}$ (68% confidence interval). The unfolded spectrum, the folded spectrum and the ratio between the data and best fit model are displayed in Fig. 6.

The ratio of the model normalizations for LECS and MECS is about 1.1, which is slightly in excess of the value expected from the known differences in the absolute calibration of the two instruments. However, given the present statistics we consider the fit acceptable. We note that using only the MECS data we obtain for the temperature $kT = 5.5^{+4.9}_{-1.75}$ (68% confidence interval), which is consistent with (and even more constrained than) that obtained by the combined (LECS + MECS) data set.

Finally, we note that ASCA (GIS + SIS) did measure a temperature of $kT = 8.1^{+3.7}_{-2.2}$ (68% confidence level) for MS 2053.7−0449 (Henry, 1999); given the large uncertainties involved (both from BeppoSAX and ASCA) the two results are obviously consistent. On the other hand they both suggest a temperature less than about 13–14 keV.

Using the best fit model parameters reported in Table 3, we derive an unabsorbed (0.3–3.5) keV flux of $f_{0.3-3.5\,keV} = (2.7 \pm 0.5) \times 10^{-13}\,\mathrm{erg\,cm^{-2}\,s^{-1}}$ (LECS normalization) or $f_{0.3-3.5\,keV} = (2.4 \pm 0.7) \times 10^{-13}\,\mathrm{erg\,cm^{-2}\,s^{-1}}$ (MECS normalization). The measured flux is lower, but consistent within the errors, than that derived from Einstein IPC data (see Table 1). Henry (1999) finds from ASCA data a flux $f_{0.3-3.5\,keV} = (3.85 \pm 0.31) \times 10^{-13}\,\mathrm{erg\,cm^{-2}\,s^{-1}}$ in perfect agreement with the EMSS.

The derived unabsorbed $2 - 10$ keV flux (computed assuming a mean value between the LECS and MECS normalizations) is $f_{2-10\,keV} = (1.9 \pm 0.5) \times 10^{-13}\,\mathrm{erg\,cm^{-2}\,s^{-1}}$, corresponding to a luminosity in the cluster rest frame of $L_{2-10\,keV} = (3.9 \pm 1.0) \times 10^{44} \mathrm{h_{50}^{-2}\,erg\,s^{-1}}$, and to a bolometric luminosity of $L_{bol} = (8.2 \pm 2.2) \times 10^{44} \mathrm{h_{50}^{-2}\,erg\,s^{-1}}$.

## 5. Discussion

In a recent work, Wu et al. (1999) have used the largest sample of clusters of galaxies with good broad band X-ray spectroscopy from the literature to discuss the $L_{bol} - T$ and the $L_{bol} - \sigma$ relationships[3]. Their sample is mainly composed by clusters at

[3] The reader is referred to Wu et al. (1999) for the comparison of their results with those from the literature, as well as for the comparison of the observed relationships and the theoretical ones. See also Sect. 3.3 in Borgani et al. (1999).

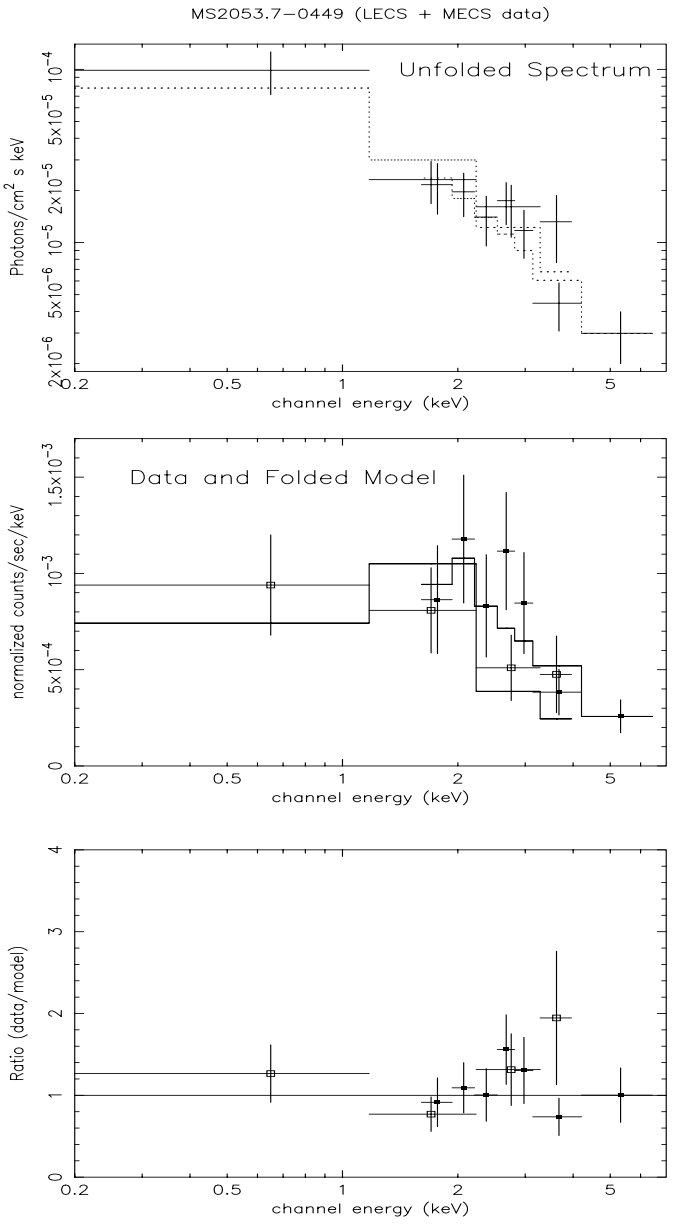


**Fig. 6.** MS 2053−0449: Unfolded spectrum, folded spectrum and the ratio between data and best fit model. In the last two panels we have indicated the LECS (MECS) data as open (filled) squares.

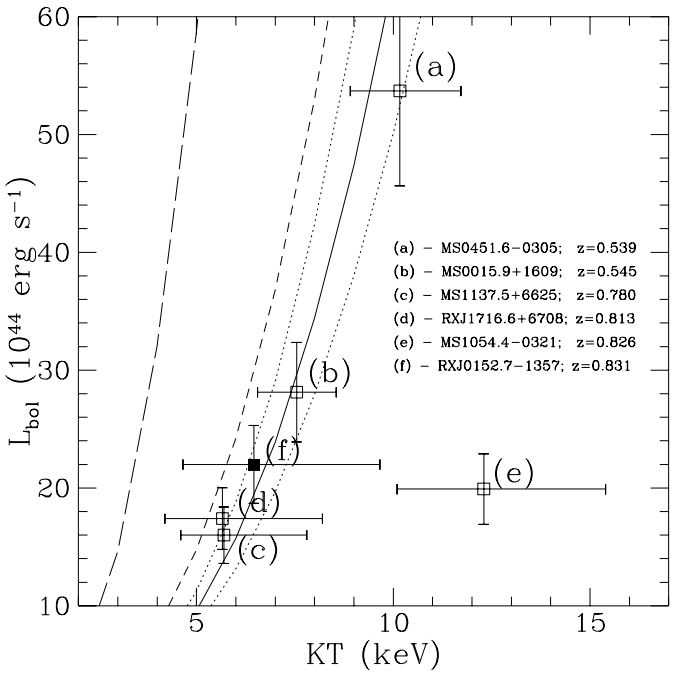


**Fig. 7.** Clusters at z $> 0.5$ with a temperature measurement (see Table 4). The filled square represents the *Beppo*SAX measured temperature of RXJ 0152.7−1357 reported in this paper. The objects have been labeled in order of increasing redshift. Error bars on the temperature represent the 90% confidence range, while error bars on the bolometric luminosity represent a realistic 15% absolute error. The solid line represents the derived $L_{bol} - T$ relationship obtained by Wu et al. (1999) using a sample of 142 clusters from the literature; the dotted lines represent the $\pm 2\sigma$ scatter on the slope. The short dashed line represents the evolving $L_{bol} - T$ relationship with $(1+z)^1$ at $z = 0.54$, while the long dashed line represents the evolving $L_{bol} - T$ relationship with $(1+z)^3$ at $z = 0.83$. See Sect. 5 for details.

$z < 0.5$ (only 5 clusters out of 142 used are at higher redshift). By comparing the clusters at $z < 0.1$ with those at $z > 0.1$ they do not find convincing evidence for a significant evolution in the $L_{bol} - T$ and the $L_{bol} - \sigma$ relationship out to $z \simeq 0.4$, a result which was first pointed out by Mushotzky & Scharf (1997).

As summarized in Table 4, distant cluster temperatures which have been measured to date are limited to a few systems at $z > 0.5$. At these redshifts the lookback time approaches half the age of the Universe and, therefore, the time leverage to measure evolution in cluster properties is large.

In Fig. 7, we plot the high redshift cluster temperatures known to date in the $L_{bol} - T$ plane. The error on the temperature represent the 90% confidence range, while we have used a realistic 15% absolute error for the bolometric luminosity. Since MS 2053.7−0449 and AXJ 2019−1127 have very large errors on the measured temperature, we have not reported these objects in Fig. 7.

The $L_{bol} - T$ relationship for clusters at $z < 0.5$ obtained by Wu et al. (1999) ($L_{bol} = 10^{-0.92\pm0.05} T^{2.72\pm0.05}$) is also shown (solid line), together with the $\pm 2\sigma$ on the slope (dotted lines). The short-dashed line represents the evolving $L_{bol} - T$ relationship with $L_{bol} \propto (1+z)^{A1}$ at $z = 0.54$, while the long dashed line represents the evolving $L_{bol} - T$ relationship with $L_{bol} \propto (1+z)^{A2}$ at $z = 0.83$. The two redshifts enclose all the objects shown in Fig. 7. For A1 and A2 we have assumed the values 1 and 3, respectively; these two values have been determined by Borgani et al. (1999), and represent the 90% confidence level required to fit the lack of observed evolution of the XLF in the RDCS cluster sample in a $\Omega_o$ = 1 universe. Low density models, instead, can easily be accommodated with a non-evolving $L_{bol} - T$ relation, or mild ($A < 1$) evolution. The new cluster temperature we have determined for RXJ0152.7−1357 is not consistent with a strong evolution of the $L_{bol} - T$ relation out to $z \sim 0.8$. Since all the data points in Fig. 7 lie to the right of the $A = 1$ line, according to the parameterization of Borgani et

**Table 4.** Clusters at $z > 0.5$ with a temperature measurement.

| Name | z | KT[a] (keV) | $L_{bol}$ $10^{44} h_{50}^{-2}$ erg s$^{-1}$ | Ref. |
|---|---|---|---|---|
| MS 0451.6−0305 | 0.539 | $10.17^{+1.55}_{-1.26}$ | 53.7 | WXF,M+S,D96 |
| MS 0015.9+1609 | 0.545 | $7.55^{+1.0}_{-1.0}$ | 28.1 | WXF,M+S,HB98 |
| MS 2053.7−0449 | 0.583 | $6.7^{+13}_{-3.1}$ | 8.2 | This paper |
| MS 1137.5+6625 | 0.78 | $5.7^{+2.1}_{-1.1}$ | 16.0 | D99 |
| RXJ 1716.6+6708 | 0.813 | $5.66^{+2.54}_{-1.46}$ | 17.4 | WXF,G99 |
| MS 1054.4−0321 | 0.826 | $12.30^{+3.10}_{-2.20}$ | 19.9 | WXF,D98 |
| RXJ 0152.7−1357 | 0.831 | $6.46^{+3.2}_{-1.8}$ | 22.0 | This paper |
| AXJ 2019−1127 | 1.00 | $8.60^{+9.5}_{-4.0}$ | 19.4 | WXF,H97 |

[a] For consistency with the other measurements we have reported in this column the 90% confidence range.
*Ref*: WXF: Wu et al. (1999); M+S: Mushotzky & Scharf (1997); D96: Donahue (1996); D98: Donahue et al. (1998); G99: Gioia et al. (1999); D99: Donahue et al. (1999); HB98: Hughes & Birkinshaw (1998); H97: Hattori et al. (1997).

al. (1999), the cluster temperatures measured so far at $z > 0.5$ lend considerable support to cosmological models with a low density parameter. Similar results have been recently obtained by Donahue et al. (1999) and by Donahue & Voit (1999). Using a complete sample of high redshift EMSS clusters, Donahue et al. (1999), have shown that the cluster temperature function reveals modest evolution, a result which implies a low $\Omega$ value (Donahue & Voit 1999).

The metal abundance of the ICM in rich clusters of galaxies has been recently investigated by Mushotzky & Loewenstein (1997). They found that the Fe abundance shows little or no evolution out to $z \sim 0.3$ ($\langle Fe \rangle \sim 0.3$), suggesting that most of the enrichment of the ICM occurred at $z > 1$. Given the present uncertainty on the ICM abundance in RXJ 0152.7−1357 we cannot set strong constraints on the cosmological evolution of the Fe abundance. However, within the large uncertainty ($A = 0.53^{+0.29}_{-0.24}$; 68% confidence interval), these data suggest that the bulk of the Fe enrichment was completed by $z \sim 1$.

Finally it is worth comparing RXJ 0152.7−1357 with MS1054.4−0321. Provided that temperature measurements are not biased by cooling flows, strong deviations from isothermality or by the presence of contaminating AGN, it is interesting to note that the temperature of MS1054.4−0321 is significantly higher than that of RXJ 0152.7−1357, although the two clusters have very similar luminosities. With the present X-ray data we are unable to discuss any further the difference in temperature between these two distant clusters which have nonetheless many similarities. The highly spatially resolved X-ray spectroscopy and high throughput that *Chandra* and XMM will provide are needed to clarify this problem as well as to study in detail distant clusters of galaxies.

## 6. Summary and conclusions

We have presented and discussed *Beppo*SAX observations of two high redshift clusters of galaxies: MS 2053.7−0449 at $z = 0.58$ and RXJ 0152.7−1357 at $z = 0.83$.

The first object has been selected from the EMSS sample. No constraints on the metallicity can be derived from the present data; by fixing the abundance to 0.3 solar we measure a gas temperature with very high uncertainty ($kT = 6.7^{+6.8}_{-2.3}$ keV).

The second cluster has been selected from the RDCS sample and is one of the most X-ray luminous system known at $z > 0.6$. It is characterized by a complex morphology (both in the optical and soft X-ray) with at least two cores, a gas temperature of $kT = 6.46^{+1.74}_{-1.19}$ keV and a metallicity of $A = 0.53^{+0.29}_{-0.24}$ (68% confidence interval). A prominent iron $K_\alpha$ line is clearly visible in the MECS spectrum.

In light of this new cluster temperature measurement at $z \sim 0.83$, we have discussed the high redshift ($z > 0.5$) $L_{bol} - T$ relationship and we have found that the limited data available so far can easily be accommodated with a non-evolving (or mildly evolving) $L_{bol} - T$ relation. This result, when combined with the little observed evolution in the X-ray cluster abundance, gives support to cosmological models with a low density parameter (e.g. Borgani et al., 1999).

*Acknowledgements.* RDC and IMG are greateful to T. Maccacaro for the continuous support and encouragement since the early phases of this work. M. Hattori provided us with unpublished data for AXJ 2019−1127. We thank G. Chincarini, C. Lobo, A. Wolter and G. Zamorani for a careful reading of the paper and useful comments. We thank the *Beppo*SAX SDC, SOC and OCC teams for the successful operation of the satellite and preliminary data reduction and screening. This research has made use of SAXDAS linearized and cleaned event files produced at the *Beppo*SAX Science Data Center. IMG acknowledges partial financial support from NSF AST95-00515, from NASA-STScI GO-06668.02-95A and from CNR-ASI grants.

## References

Boella G., et al., 1997, A&AS 122, 327
Borgani S., Rosati P., Tozzi P., Norman C., 1999, ApJ 517, 40
Burke D.J., Collins C.A., Sharples R.M., Romer A.K., Holden B.P., Nichol R.C., 1997, ApJ 488, L83
Chiappetti L., Cusumano G., Del Sordo S., et al., 1998, in "The Active X-ray Sky", L. Scarsi, H. Bradt, P. Giommi, F. Fiore (Eds.), Nuclear Physics B Proc. Suppl. 69/1-3, 610
Clowe D.I., 1998, PhD Thesis, University of Hawaii
Clowe D.I., Luppino G.A., Kaiser N., Gioia I.M., 1999, ApJ, submitted.
Crawford C.S., Fabian A.C., 1996, MNRAS 282, 1483

Deltorn J-M., Le Fèvre O., Crampton D., Dickinson M., 1997, ApJ 483, L21
Dickey J.M., Lockman F.J., 1990, ARAA 28, 215
Dickinson M.D., 1997, in "The Early Universe with the VLT", Ed. J. Bergeron, Berlin, Springer, p. 274
Donahue M., 1996, ApJ 468, 79
Donahue M., Voit G.M., Gioia I.M., Luppino G.A., Hughes J.P., Stocke J.T., 1998, ApJ 502, 550
Donahue M., Voit G.M., Scharf C.A., Gioia I.M., Mullis C.R., Hughes J.P., Stocke J.T., 1999, ApJ, in press, astro-ph/9906295
Donahue M., Voit G.M., 1999, ApJ 523, L137
Ebeling H., et al., 1999, ApJ, submitted.
Eke V.R., Cole S., Frenk C.S., 1996, MNRAS 282, 263
Fiore F., Guainazzi M., Grandi P. 1999, technical report, ftp://www.sdc.asi.it/pub/sax/doc/software_docs/saxabc_v1.2.ps.gz
Frontera F., Costa E., Dal Fiume D., et al., 1997, A&AS 122, 357
Gioia I.M., Luppino G.A., 1994, ApJS 94, 583
Gioia I.M., Maccacaro T., Schild R.E., et al., 1990, ApJS 72, 567
Gioia I.M., Henry J.P., Mullis C.R., Ebeling H., Wolter., A. 1999, AJ 117, 2608
Hattori M., Ikebe Y., Asoaka I., et al., 1997, Nature 388, 146.
Henry J.P., Gioia I.M., Maccacaro T., et al., 1992, ApJ 386, 408
Huges J.P., Birkinshaw M., 1998, ApJ 501, 1
Henry J.P., 1999, ApJ, submitted.
Kelson D.D., van Dokkum P.G., Franx M., Illingworth G.D., Fabricant D., 1997, ApJ 478, L13
Luppino G.A., Gioia I.M., 1992, A&A 265, L9
Luppino G.A., Gioia I.M., Hammer F., Le Fèvre O., Annis J.A., 1999, A&AS 136, 117
Manzo G., Giarrusso S., Santangelo A., et al., 1997, A&AS 122, 341
Mullis C.R. Gioia I.M., and Henry J.P., 1998, IAU Symposium 188 "The Hot Universe", Eds. K. Koyama, S. Kitamoto, M. Itoh, pages 473–474
Mushotzky R., Loewenstein M., 1997, ApJ 481, L63
Mushotzky R., Scharf C., 1997, ApJ 482, L13
Navarro J.F., Frenk C.S., White S.D.M. 1996, ApJ 462, 563
Oke J.B., Cohen J.G., Carr M., et al., 1995, PASP 107, 375
Parmar A.N., Martin D.D.E., Bavdaz M., et al., 1997, A&AS 122, 309
Parmar A.N., Oosterbroek T., Orr A., et al., 1999, A.A. Suppl. 136, 407
Peebles P.J.E., Daly R., Juskeiewicz R., 1989, ApJ 347, 563
Press W., Schechter P., 1974, ApJ 187, 425
Raymond J.C., Smith B.W., 1977, ApJS 35, 419
Romer A.K., Nichol R.C., Holden B.P., et al., 1999, astroph-9907401.
Rosati P., Della Ceca R., Burg R., Norman C., Giacconi R., 1995, ApJ 445, L11
Rosati P., Della Ceca R., Norman C., Giacconi R., 1998, ApJ 492, L21.
Rosati P., Stanford A.S., Eisenhardt P.R., et al., 1999, AJ 118, 76
Scharf C.A., Jones L.R., Ebeling H., et al., 1997, ApJ 477, 79
Smail I., Dickinson M., 1995, ApJ 455, L99
van Haarlem M.P., Frenk C.S., White S.D.M, 1997, MNRAS 287, 817
Vikhlinin A., McNamara B.R., Forman W., et al., 1998, ApJ 502, 598
Wu X-P., Xue Y-J., Fang L-Z., ApJ 524, 22.